IOP Conf. Series: Materials Science and Engineering **360** (2018) 012017 doi:10.1088/1757-899X/360/1/012017

# EFFECT OF TEMPERATURE ON THE OPTICAL AND ANTIOXIDANT PROPERTIES OF BIO AND ORGANIC SYNTHESISED HEMATITE NANOPARTICLES

Malu Somaraj[1*], Nancy John[1], Nisha J Tharayil[2] and S. Usha[3]

[1]*Department of Physics, S.N College, Kollam, Kerala, India*

[2]*Department of physics, S.N College for Women, Kollam, Kerala, India*

[3]*Department of Zoology, S.N College for Women, Kollam, Kerala, India*

**Corresponding author*

*Email:* ***malusandram@gmail.com***

Phone Number: +919446832451

**Abstract:** The hematite nanoparticles with tunable band gap were synthesised through a simple and novel co-precipitation technique using bio (DNA) and organic (EDTA) templates. The obtained precursor was heated on the basis of TGA to obtain the metal oxide nanoparticles. The crystalline and morphological changes during heat treatment of synthesised sample were discussed using XRD, SEM and TEM analysis. The optical characterisations were done using UV-Vis spectroscopy and FTIR studies. The invitro antioxidant study of samples treated at two different temperatures using DPPH assay provide the possibility of improving radical scavenging activity by varying the preparation conditions.

## 1. Introduction

Nanosized iron oxides are of tremendous interest when compared with their bulk counterpart due to their high surface area, high rate of reactivity and biocompatibility. They have superior characters in nontoxicity, Chemical stability, durability, and low costs [1]. Among different iron oxide nanoparticles, Hematite ($\alpha$-$Fe_2O_3$) is the most stable polymorph in nature under ambient condition and it can be easily found as mineral hematite. Nanostructured $\alpha$-$Fe_2O_3$ powders have been prepared by different preparation techniques like sol-gel [2], hydrothermal [3], chemical vapour phase deposition [4], calcinations of hydroxides [5], radio frequency sputtering [6], gas condensation technique [7] and high energy ball-milling process [8, 9]. In this work, we describe a simple co-precipitation method for synthesising nanosized $\alpha$-$Fe_2O_3$ particles.

High surface area to volume ratio of the nanoparticles generates surfaces with very high free energy content. For reducing this energy, surface cooperate with interactomes present in cell, and become mostly stable one. But, some interactions have the energy to overcome band gap barrier of the nanoparticles, resulting into generation of electron-hole pair. The free electron, in biological system, results in production of free reactive oxygen species [10]. Moreover, intact iron oxide nanoparticles upon contact with air lose its magnetism and monodispersibility [11]. To avoid such problems, various research groups have taken the help of different chemical and biological agents to modify the surfaces, and stop the lose. In our

work, DNA, a bio- template and EDTA, an organic- template were chosen to coat hematite nanoparticles surface. Reduction of the particle size to nanometer range is accompanied by altered electrical, magnetic, electro-optical and chemical properties. Usually, these special properties are caused by the changes of the band structure with decrease of the particle size, which is usually called the quantum-confinement effect. However, as a larger fraction of the atoms in the particles comprises surface atoms, the surface layer has a significant influence on the properties of these nanoparticles. Hematite ($\alpha$-$Fe_2O_3$) nanoparticles have a small exciton Bohr radius with favourable bandgap of 2.1-2.2 eV. The surface effect became the predominant in determining the optical properties of the nanosized $\alpha$-$Fe_2O_3$ particles.

The high surface to volume ratio of nanostructures makes it viable candidates to act as free radical scavengers than their bulk counter parts [12].The antioxidant assessment of nanomaterials has become a crucial study in pharmaceutical science as well as nanotechnology [13]. There are previous reports on the free radical scavenging by ZnO [12] and NiO [14] nanoparticles. Also, Das et al. [13] has reported on the antioxidant activity of CuO nanoparticles. All these encouraged our present work where we studied the antioxidant activity of bio and organic synthesised Hematite nanoparticles to get an insight about the behaviour and interaction of these materials with biomolecules inside a living system.

## 2. Materials and methods

The chemicals used in the present investigation were of Analytical Reagent (AR) grade and obtained from Merck.

### 2.1 Synthesis of $\alpha$-$Fe_2O_3$ Nanoparticles

To synthesis $\alpha$-$Fe_2O_3$ 0.1M solution of ferric nitrate and 0.4 M solution of sodium hydroxide were added drop wise into 0.01wt. % of DNA solution under constant stirring of 5 hours using a magnetic stirrer. Here DNA powder was used as capping agent to control the particle size. A reddish coloured precipitate is formed at the end of the reaction. The obtained precipitate was washed several times using distilled water to remove the impurities. The precipitate was filtered, dried in a hot air and then ground into fine powder. The same procedure was repeated with EDTA instead of DNA to get the other sample. Thus for this work we were used two different capping agents namely DNA and EDTA for the preparation of $\alpha$-$Fe_2O_3$ nanoparticles.

### 2.2 Antioxidant activity test

The radical scavenging activity of hematite nanoparticles are determined using DPPH assay. The DPPH radical scavenging activity was measured as per the process described by Blois et al [15]. 0.1mM solution of DPPH solution in methanol was prepared and 1ml of this solution was mixed with 3ml of sample solutions in methanol at different concentrations. The violet colour of DPPH radical solutions becomes colourless in presence of nanoparticles. After 30 minutes, the absorbance was measured at 517nm. Buthylated hydroxyanisole (BHA) was used as standard. Decreasing of the DPPH solution absorbance indicates an increase of the DPPH radical-scavenging activity. DPPH radical-scavenging activity was calculated using the equation

$$\% \text{ Inhibition} = ((A_0 - A_1) / A_0 \times 100) \quad (1)$$

Where $A_0$ was the absorbance of the control (1ml of DPPH + 3ml of methanol) and $A_1$ was the absorbance of the sample solution.

## 3. Characterisation

The annealing temperature is determined by the thermo gravimetric analysis (TGA). The TGA is done in a Perkin-Elmer model Diamond TG/DT instrument in the temperature range 28-800° C at a heating rate of 15° C/minute under nitrogen atmosphere. There is no further weight loss after reaching the temperature 450° C. Hence to obtain the oxide nanoparticles, the precursors were heated in a muffle furnace at 500° C for 3 hrs. X-ray diffraction (XRD) spectra of samples were recorded with a PAN Analytical Model X'pert pro X-ray diffractometer employing $Cuk_{\alpha}$ radiation at 40 KV and 100 mA at a scanning rate of 8° $min^{-1}$ in the range 20 - 80°. The surface morphology of the samples were recorded with a Hitachi-model S-3000H scanning electron microscopy and Transmission electron microscopy (TEM). The absorption spectra of the materials were taken at room temperature with the help of a Jasco V 550UV/Vis-NIR spectrophotometer. The FTIR studies of all the samples were carried out in a Perkin-Elmer FTIR Spectrophotometer between 300 $cm^{-1}$and 4000 $cm^{-1}$. The radical scavenging activities of samples were elucidated spectrophometrically using UV-1601 schimadzu spectrometer.

## 4. Results and Discussion

### 4.1 Structural Characterisation

To study the thermal effects the bio (FD) and organic (FE) synthesised powder was heated 500℃ and 700° C for 3 hours. The two samples are hereafter referred as FE1 and FD1 (heated at 500℃) and FE2 and FD2 (heated at 700° C).The crystal structure of samples prepared were characterised through X-ray diffraction and the obtained pattern shows the formation of rhombohedral phase of α-$Fe_2O_3$ (Hematite) with no characteristic peaks of other impurities. The X-ray diffraction spectrum of hematite nanoparticles annealed at 500℃ and 700° C with prominent reflecting planes is shown in the figure 1.

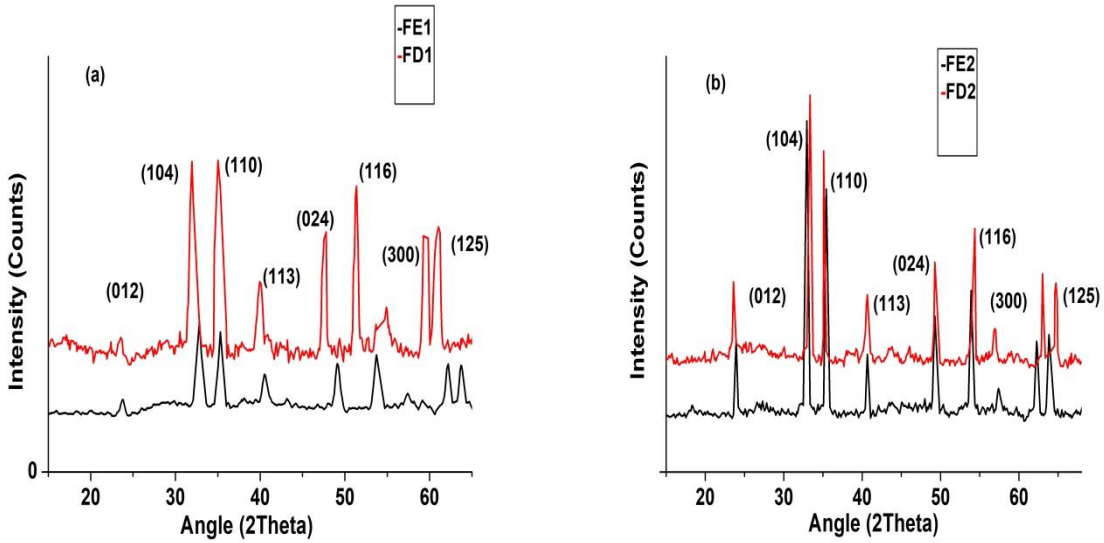


**Fig. 1. XRD spectrum of samples FE and FD a) at 500℃ and b) at 700° C**

**Table 1. Parameters obtained from XRD of samples with particle size**

| Sample | h k l | $d_{observed}$ | $d_{jcpds}$ | Particle size (avg) |
|---|---|---|---|---|
| **FE1** | 104<br>116<br>110 | 2.72745<br>2.53993<br>1.70377 | 2.7237<br>2.5560<br>1.7110 | 16.12 nm |
| **FE2** | 104<br>116<br>110 | 2.71683<br>2.53242<br>1.69970 | 2.7237<br>2.5560<br>1.7110 | 35.02 nm |
| **FD1** | 104<br>116<br>110 | 2.72598<br>2.54001<br>1.70332 | 2.7237<br>2.5560<br>1.7110 | 17.86 nm |
| **FD2** | 104<br>116<br>110 | 2.71613<br>2.53116<br>1.69986 | 2.7237<br>2.5560<br>1.7110 | 28.6 nm |

This broadening of the peaks could also arise due to microstrain of the crystal structures arising from defects like dislocations and twinning. These are believed to be associated with the nanocrystals synthesised chemically as they grow spontaneously and chemical ligands get less time to diffuse to an energetically favourable site. The XRD spectrum of samples (Table 1) were studied in detail, and compared with reported JCPDS values. The relative crystalline sizes were determined from the XRD line broadening using Scherrer equation [16]. The crystalline size of the samples FE1 and FD1 are 17.86 nm and 16.12 nm and it increases as a result of sintering to 35.02nm and 28.6 nm. This indicates that the size of the crystallites can be adjusted by controlling the temperature of the reaction [17]. The elastic strain of the material is calculated using the equation (1)

$$e = [(\lambda / D \cos \theta) - \beta] (1 / \tan \theta) \quad (2)$$

Here D is the crystallite size and β full width at half maximum of the peak with diffracting angle θ. The elastic strain is obtained as $3.877\times10^{-4}$ for sample FE1 and $3.84\times10^{-4}$ for sample FD1. This strain contributes to the broadening of XRD pattern.

### 4.2 Morphological studies

The general morphologies of Hematite nanoparticles were examined using TEM and SEM. Figure 2 shows the TEM images of the sample FE and FD which confirmed that the synthesised product are nanoparticles. The particles are nearly spherical, agglomerated and dumbbell in shape. The particle size calculated from XRD and that determined from a TEM are often different. This is because of the fact that Peak broadening may also be caused by other reasons, such as inhomogeneous strains, twinned structure, lattice bending or other point defects that may be present in the sample; hence Scherrer's equation may produce results that are different from the actual size [18]. The mean size of the particles FE1 and FD1 at 500˚C are 17.10nm and 13.6nm and at 700℃ are 77.35nm and 23.39nm respectively. The

homogeneity in shape and size of the green synthesised nanoparticles appears to be better than that of nanoparticles obtained using EDTA. It was observed that DNA can reduce the size of hematite nanoparticles as varying the temperature. The morphology of the hematite nanoparticles was not uniform, formation of large cluster and particle agglomeration resulting increased particle size was observed [19, 20].

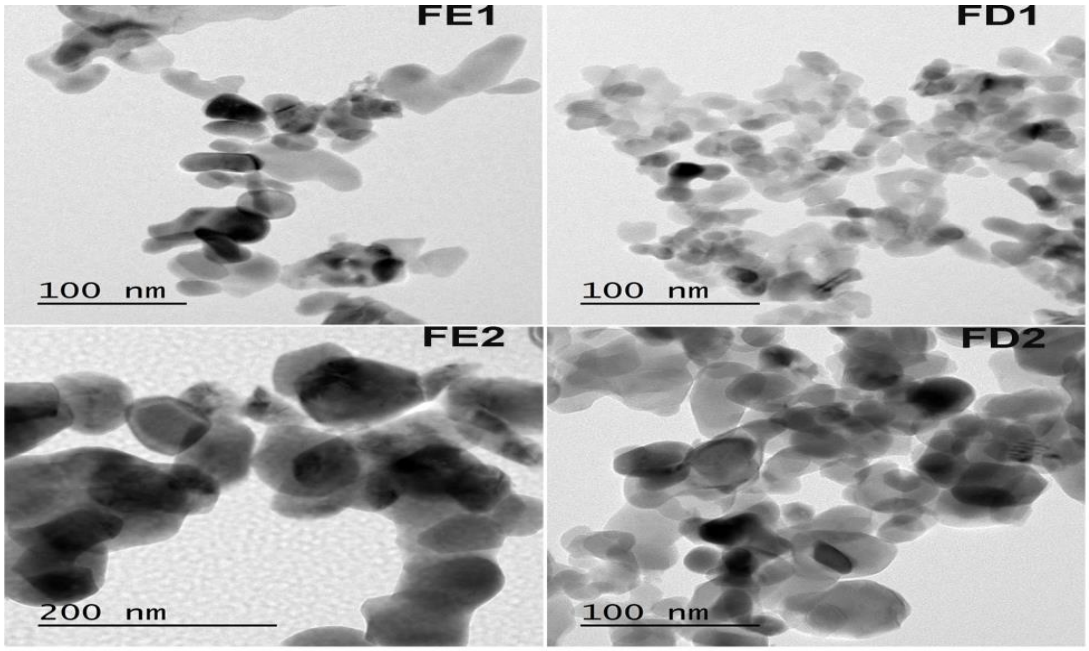


**Fig. 2.TEM images of sample FE and FD**

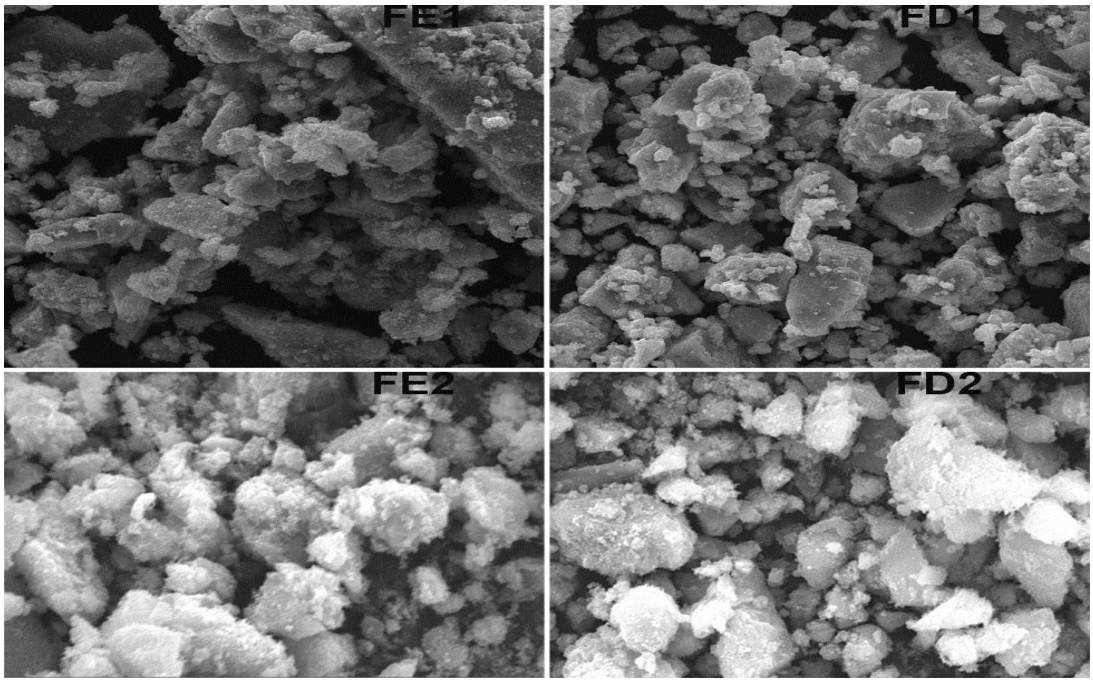


**Fig. 3.SEM images of sample FE and FD**

The hematite nanoparticles were found be to be aggregated into larger irregular structures with no well-defined morphologies. The agglomeration of nanoparticles is generally explained as common way to minimize their surface free energy; but some studies reported that the agglomeration is assigned to the existence of organic radicals that act as binders [21].

### 4.3 Absorption studies

### UV-Visible spectroscopy

Figure 4 presents the UV-visible absorption spectra of the samples FE and FD annealed at 500° C and 700° C. The absorbance spectra of the two samples were composed of several absorption bands, whose positions were in good agreement with the expected absorption bands of octahedral $Fe^{3+}$. In fact, according to previous studies, the UV-visible absorption spectrum of hematite was composed of four intense bands located near 230, 290, 345 and 395 nm, with the major absorption being located between 210 and 230 nm [22]. All these absorption bands are due to $Fe^{3+}$ -$O^{2-}$ charge transfer.

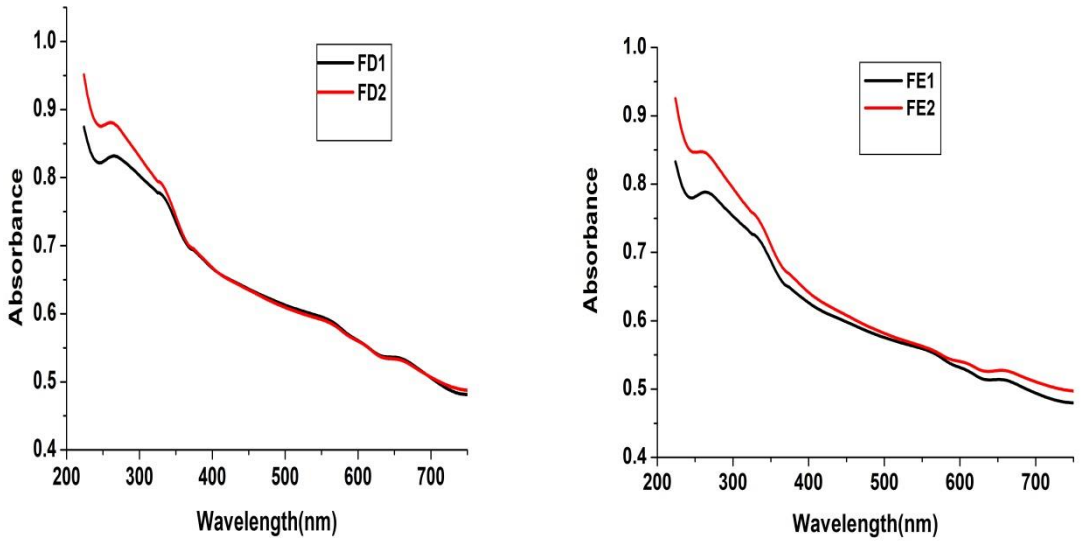


**Fig. 4. UV-visible absorption spectra of the samples FD and FE at 500° C and 700° C**

The presence of a blue shift of the absorption bands as the annealing temperature decreases and the consequent decrease of crystalline size was observed in this work. This blue shift can be quantified by calculating the experimental band-gap value from the absorption spectra. Moreover Hematite is an n-type semiconductor [23]. The band gap value, Eg, was determined from UV-visible absorption spectra using the relation between the absorption coefficient, α, and the energy of the incident light, hν

$$\alpha h\nu = A(h\nu - Eg)^n \quad (3)$$

e A is a constant, hν the photon energy, Eg the energy gap and n is an index which assumes different values depending on the nature of electronic transitions possible. As it was indirect transition n was taken as 2 and the graph between $(\alpha h\nu)^2$ and hν is shown in Figure 5. The intersection of the extrapolated linear portion with the abscissa axis gives the band-gap value. The band gap values were 3.85eV and 3.39eV for sample FE and 3.86 eV and 3.72eV for sample FD annealed at 500° C and 700° C. The observed values are higher and blue shifted from the reported value of bulk hematite because of the quantum size confinement in the nanoparticles.

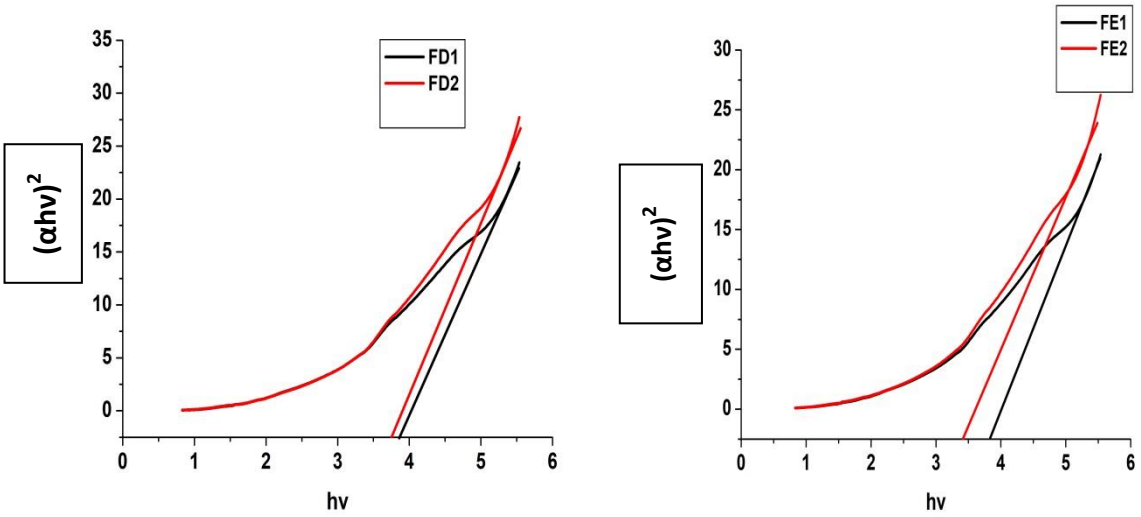


**Fig. 5. Tauc plot to evaluate bandgap of FD and FE**

## FTIR analysis

The FTIR spectrum is a fingerprint of the structure and shows the formation of metal oxides. Two main broad metal-oxygen bands were seen in the FTIR spectrum (Fig 6) of hematite nanoparticles. The highest one $\nu_1$observed around 534 $cm^{-1}$ corresponds to intrinsic stretching vibration of the, Fe↔O, whereas the lowest band, usually observed around 449-454 $cm^{-1}$ is assigned to bending vibration of the O↔Fe↔O [24]. Due to the nano size of the grains the IR active modes slightly shifts due to the difference in coordination number and bond length but still the bands around 400 $cm^{-1}$ and 500 $cm^{-1}$ are typical metal oxides. The peak centered at 3383- 3428 $cm^{-1}$ corresponds to the stretching vibration of intermolecular hydrogen bond (O-H) existing between the adsorbed water molecules and indicates the lower amount of hydroxyl group. The FTIR peaks at 1619-1630 $cm^{-1}$ corresponds to the surface absorbed water. The IR spectrum of FD sample shows an extra peak around 900-1000 $cm^{-1}$ which was the signature of deoxyribose region [25]. This indicates the interaction of DNA with Hematite particles. All the peaks in the samples FD and FE are gradually diminished as the annealing temperature increased. The FTIR results obtained in this study were coinciding well with the XRD analysis where, both analyses showed the synthesised samples are nanosized hematite.

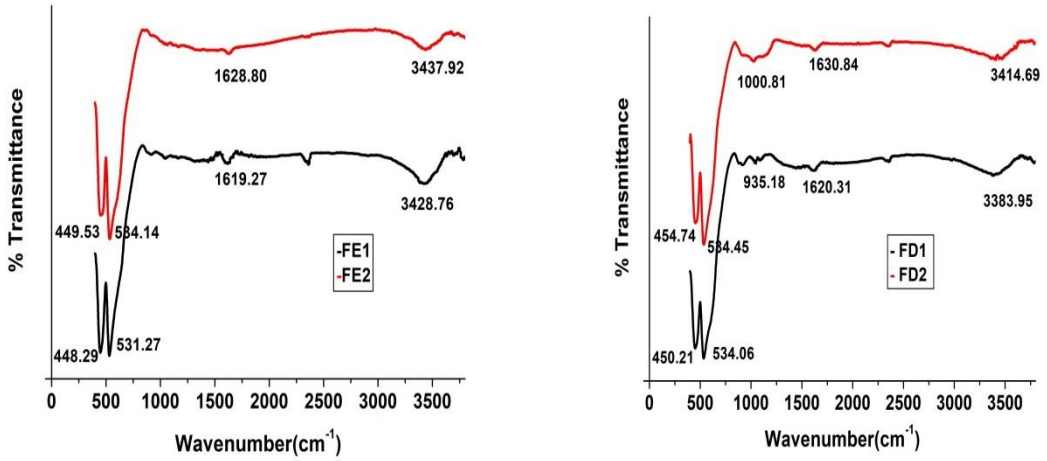


**Fig. 6. FTIR spectrum of samples FE and FD**

### 4.4 Antioxidant Activity

The antioxidant activities of the samples (FE and FD) were validated using DPPH assay. Antiradical activity assay was based on the reduction of 1, 1-diphenyl-2-picrylhydrazyl (DPPH). Due to the presence of an odd electron it gives a strong absorption maximum at 517nm.The scavenging effect of samples at 500℃ and 700℃ on DPPH radical is investigated and the variation of optical density with concentration graph showing the result on comparison with the standard is presented in fig 7. The antioxidant efficiency was found to increase with the increase of sample dosage for both samples [26-27] shown in table 2.

**Table. 2. Antioxidant activity of samples FE and FD**

| Concentration (µg) | Antioxidant activity (%) | | | |
|---|---|---|---|---|
| | FE1 | FD1 | FE2 | FD2 |
| 10 | 7.5 | 9 | 14 | 8.7 |
| 30 | 11.8 | 13 | 14.8 | 10.2 |
| 50 | 16.7 | 20 | 14.8 | 10.6 |
| 70 | 22.7 | 30 | 14.7 | 11.5 |
| 90 | 23.6 | 31 | 14.8 | 19.9 |
| 100 | 30.6 | 31 | 14.8 | 25 |

It can be noticed that the annealed samples (at 700℃) FD2 and FE2 exhibits a lower scavenging activity when compared to the samples FD1 and FE1 annealed at 500℃. The decrease in activity with increase in annealing temperature can be attributed to the decrease in surface area to volume ratio due to increased crystalline size. The scavenging activity exhibited by nano sized hematite can also be attributed to the ability of Hematite

nanoparticles to transfer its electron density towards the free radical located at nitrogen atom in DPPH.

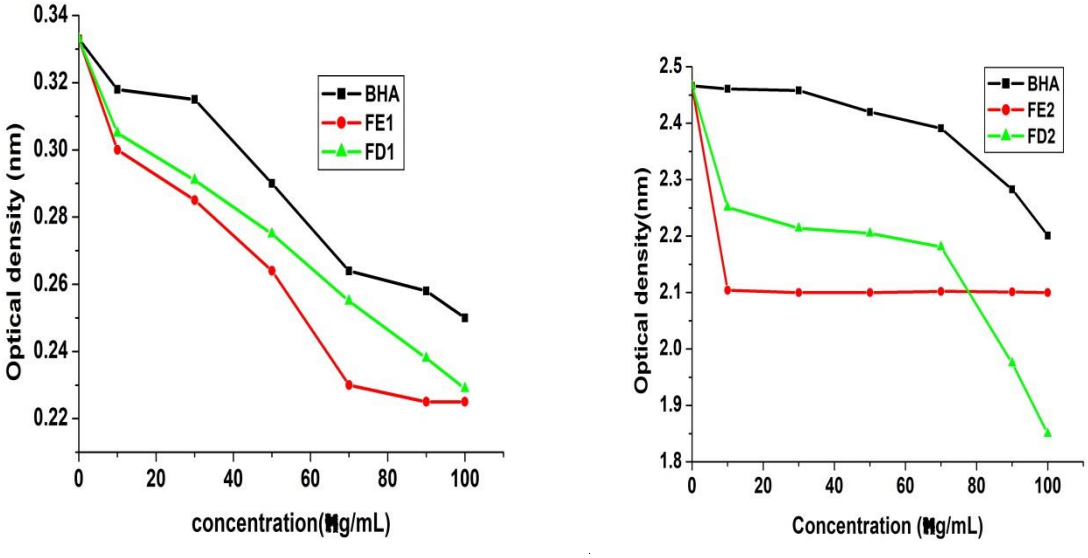


**Fig. 7. Optical density-concentration graph for DPHH scavenging activity of samples FE and FD**

## 5. Conclusion

Nanosized hematite with different crystalline sizes was successfully elaborated via co-precipitation method using bio and organic template. The XRD measurements revealed that the sample was nano sized hematite. The morphology, shape and size of the crystals improved on annealing. Compared to EDTA, DNA can be used as an effective capping agent to reduce the size of hematite nanoparticles even on annealing. This fact was confirmed from XRD and TEM measurements. The influence of crystalline size on optical properties relating to absorption was strongly confirmed. Radical scavenging activity of hematite nanoparticles showed good result at lower annealing temperature. The antioxidant activity of the prepared metal oxide nanoparticles proves it to be a potential member of bioactive materials. It is concluded that further exploration on this field needed to develop eco-friendly bio-nanomaterials for biomedicines.

## Acknowledgement

The authors are pleased to acknowledge STIC, Cochin for XRD, SEM and TEM imaging. The help rendered by CEPC, Kollam for antioxidant study is thankfully acknowledged.

## References

1. M. A. Legodi and D. De Waal, *Dyes and Pigments*.1, 74 **(2007)**

2. R. Pascual, M. Sayer, C. V. R. V. Kumar, and L. Zou, *J.Appl. Phys*. 4, 70 **(1991).**

3. X. Wang, X. Chen, X. Ma, H. Zheng, M. Ji, and Z. Ahang, *Chem. Phys. Lett.* 4-6,384 **(2004).**
4. E.T. Kim and S.G. Yoon, *Thin solid Films*. 1, 227 **(1993)**.
5. X. Bokhimi, A. Morales, M. Portilla, and A. Garcia-Ruiz, *Nanostruct. Mater.* 1, 12 **(1999)**.
6. W. G. Luo, A. L. Ding, X. T. Chen, and H. Li, *Integrated Ferroelect.* 9 **(1995)**.
7. R. Birringer, H. Gleiter, H. P. Klein and P. Marquardt, *Phys. Lett.A.8,102* **(1984)**.
8. D. Michel, E. Gaffet, and P. Berthet, *Nanostruct. Mater.* 5-8, **(1995)**.
9. M. Chakrabarti, D. Bhowmick, A. Sarkar, *J. Mater. Sci.*19, 40 **(2005)**.
10. M. Arakha, M. Saleem, B. C. Mallick & S. Jha, Sci rep 5, doi: 10.1038/srep09578 **(2015)**.
11. M. Mahdavi, *Molecules*.18 **(2013).**
12. D. Das, B.C. Nath, P. Phukon, A. Kalita, S. K. Dolui, *Colloids Surf. B.* 111 **(2013).**
13. . Das, B.C. Nath, P. Phukon, A. Kalita, S. K. Dolui, *Colloids Surf. B.* 101 **(2013).**
14. J. P. Saikaia, S. Paul, B. K. Konwar, S. K. Samdarshi, *Colloids Surf. B.* 78 **(2010)**.
15. M. S Blois M S, *Nature.* 181**(1958).**
16. Harol P Klug & Leroy E Alexander, X-ray powder diffraction procedure, John Wiley & Sons, New York **(1954).**
17. L. P. Wang, Hong G. Y, S. C Qu & Z.G Wang, *Nanotech.* 16 **(2005).**
18. Nisha J Tharayil, S. Sagar, R. Raveendran and A.V. Vaidyan, Physica B. 399 **(2007)**.
19. K.J. Sreeram, M. Nidhin, B.U Nair, *Colloids and Surfaces B: Biointerfaces.*71 **(2009)**.
20. K.J. Sreeram, M. Nidhin, B.U Nair, *Appl. Surf.* Sci. 258, **(2012)**.
21. N. Dhananjaya, H.C Nagabhushana, R.P.S Chakradhar, R.P.S, *J. Alloys and Compounds.* 509 **(2011)**.
22. E. A. Cloutis, K. A. McCormack, J. F. Bell, III, A. R. Hendrix, D. T. Bailey, M. A. Craig, S. A. Mertzman, M. S. Robinson, and M. A. Riner, *Icarus*. 197 **(2008).**
23. S. Zeng, K. Tang, and T. Li, *J. Colloid Interface Sci.* 312 **(2007).**
24. M. Salavati-Nissari, F. Davar, T. Mahmoudi, *Polyhedron.* 28 **(2009).**
25. Debasish Sarkar, Kalyan Mandal and Madhuri Mandal, *Nanosci. and Nanotech. Lett*. 3 **(2011).**

26. R. Bungheza, E. Barbinta patrascuc, Badead M Donceaa, Popescuc M Iona, *J. optoelect. and advanced mater.* 14 **(2012).**

27. Amit Kumar Mittal, Abhishek Kaler, Uttam Chand Banerjee, Nano Biomed.and Eng, 4 **(2012).**